J. Mol. Biol. (1978) **118**, 365–388

*Eco*RI Analysis of Bacteriophage P22 DNA Packaging

ETHEL NOLAND JACKSON, DAVID A. JACKSON AND ROBERT J. DEANS

Department of Microbiology, The University of Michigan Medical School Ann Arbor, Mich. 48109, U.S.A.

(Received 18 May 1977, and in revised form 9 September 1977)

Bacteriophage P22 linear DNA molecules are a set of circularly permuted sequences with ends located in a limited region of the physical map. This mature form of the viral chromosome is cut in headful lengths from a concatemeric precursor during DNA encapsulation. Packaging of P22 DNA begins at a specific site, which we have termed *pac*, and then proceeds sequentially to cut lengths of DNA slightly longer than one complete set of P22 genes (Tye *et al.*, 1974*b*). The sites of DNA maturation events have been located on the physical map of *Eco*RI cleavage sites in P22 DNA. *Eco*RI digestion products of mature P22 wild-type DNA were compared with *Eco*RI fragments of two deletion and two insertion mutant DNAs. These mutations decrease or increase the length of the genome, but do not alter the DNA encapsulation mechanism. Thus the position of mature molecular ends relative to *Eco*RI restriction sites is different in each mutant, and comparison of the digests shows which fragments come from the ends of linear molecules. From the positions of the ends of molecules processed in sequential headfuls, the location of *pac* and the direction of encapsulation relative to the P22 map were deduced. The *pac* site lies in *Eco*RI fragment A, $4{\cdot}1 \times 10^3$ base-pairs from *Eco*RI cleavage site 1. Sequential packaging of the concatemer is initiated at *pac* and proceeds in the counterclockwise direction relative to the circular map of P22. One-third of the linears in a population are cut from the concatemer at *pac*, and most packaging sequences do not extend beyond four headfuls.

Fragment D is produced by *Eco*RI cleavage at a site near the end of a linear chromosome which has been encapsulated starting at *pac*. The position of the *pac* site is therefore defined by one end of fragment D. The *pac* site is not located near genes *12* and *18*, the only known site for initiation of P22 DNA replication, but lies among late genes at a position on the physical gene map approximately analogous to the cohesive end site (*cos*) of bacteriophage λ at which λ DNA is cleaved during encapsulation. Our results suggest that P22 and λ DNA maturation mechanisms have many common properties.

1. Introduction

Each P22 bacteriophage particle contains a single molecule of linear, double-stranded DNA. The mature linear P22 DNA molecules isolated from a population of virus particles are circularly permuted and terminally redundant (Rhoades *et al.*, 1968; Tye *et al.*, 1974*a*,*b*). Streisinger *et al.* (1967) first suggested how circularly permuted, terminally redundant chromosomes could be generated during phage DNA encapsulation. Streisinger proposed that the intracellular precursor to the mature DNA is a concatemer, and the length of DNA cut from the concatemer equals the amount of DNA which will fit into the phage head, or one "headful". The length of one DNA

headful can accommodate slightly more than one complete set of phage genes. Thus this headful encapsulation mechanism, cutting the concatemer either randomly or sequentially, will generate circularly permuted, terminally redundant linear DNA molecules.

Tye *et al.* (1974*b*) showed that mature P22 DNA molecules are formed during DNA encapsulation by a variation of the headful mechanism described by Streisinger. When circularly permuted and terminally redundant P22 DNA molecules were analyzed in the electron microscope after partial denaturation, the ends of these linear molecules were found to fall over less than 20% of the partial denaturation map. Tye *et al.* (1974*b*) proposed that this limited set of circularly permuted chromosomes could be produced by headful packaging of DNA if encapsulation begins at a specific site on the P22 DNA concatemer (Botstein & Levine, 1968) and proceeds sequentially in one direction along the concatemeric precursor. A DNA encapsulation mechanism which begins at one site and cuts a limited number of sequential headfuls will produce terminally redundant, circularly permuted linear DNA molecules all having ends within a limited region of the genome if the terminal redundancy is small.

The experiments of Tye *et al.* (1974*a*,*b*) showed that, once encapsulation begins at the packaging initiation site, cutting of the concatemer by the headful packaging mechanism shows no site specificity. Partial denaturation mapping demonstrated that the presence of a large deletion or insertion in P22 DNA, which decreases or increases the length of the genome relative to the size of the headful, yields mature linear chromosomes with ends falling in all regions of the genome. Therefore, after the initial packaging event that begins a sequence of headfuls at a unique genetic location, the encapsulation mechanism can cut P22 DNA without any site specificity.

To generate the physical map of the P22 chromosome reported here and in the preceding paper, mature P22 DNA molecules were digested to a limit product with the restriction enzyme *Eco*RI. Digestion of linear P22 DNA produces fragments which can be separated by agarose gel electrophoresis to form eight bands. Several of these bands are unusual: the band migrating most slowly contains fragments that are quite heterogeneous in molecular weight, another band contains a fragment present in greatly reduced molar yield, and the molar yields of two other fragments are somewhat reduced. In contrast, restriction enzyme digestion of most viral DNAs, including DNA of the related bacteriophage λ, yields a set of discrete fragments present in equimolar amounts. The experiments reported here show that the anomalies in the P22 *Eco*RI fragment pattern are consequences of the limited circular permutation of P22 DNA and the mechanism by which concatemeric precursor DNA is matured and packaged.

In the accompanying paper (Jackson *et al.*, 1978), seven of the eight fragments produced by digestion of P22 DNA by *Eco*RI were ordered. However, those experiments gave no information about the origin of the eighth fragment (fragment D), or about the anomalies in the fragment pattern. In this paper, *Eco*RI digests of mature DNA of several P22 deletion and insertion mutants are compared with the wild-type P22 digestion products. These mutations alter the genome size, but not the packaging mechanism, so that the ends of permuted linear molecules fall in different regions of the physical map (Tye *et al.*, 1974*b*). By considering the fragments produced by *Eco*RI cleavage of the ends of these linears, we were able to infer the positions of maturation cleavages of the concatemeric DNA precursor relative to P22 *Eco*RI sites. Here we confirm that P22 DNA can be depicted as a circular array

of seven *Eco*RI cleavage sites. We determine the physical location of ends of mature linear molecules of the wild-type P22 DNA and the deletion and insertion mutants. From these results we construct maps of the physical locations of DNA maturation events on wild-type P22 DNA and the insertion and deletion DNAs. The description of P22 DNA packaging contained in these maps defines the origin of fragment D and accounts for all the other anomalous features of an *Eco*RI digest of mature P22 DNA. Our results confirm by a different method the view of P22 DNA packaging proposed by Tye *et al.* (1974*b*) and provide more detailed information about the packaging process.

2. Materials and Methods

(a) *Bacterial and bacteriophage strains*

P22 Tc-10 carries an insertion of genetic material which includes genes determining tetracycline resistance (Watanabe *et al.*, 1972; Chan *et al.*, 1972; Tye *et al.*, 1974*a*). Each particle of P22 Tc-10 is defective, since the complete genome will not fit into one P22 head. The complete genome of P22 Tc-10 *tet*^{R} c2-*ts*30, used here, was maintained in the prophage state and thermally induced to yield defective phage particles from which linear DNA was extracted. P22 bp1 *tet*^{R} *Δ*[*att int*] and P22 bp5 *Δ*[*att int*] are non-defective deletion revertants of P22 Tc-10 (Tye *et al.*, 1974*a*, Chan & Botstein, 1976). The prophage attachment site and integration gene are removed by the deletion in each phage. Both strains retain part of the *tet*^{R} insertion. The P22 bp5 strain used carried a clear plaque mutation (c2-*am*O8), and a lysis mutation (13^{-}*am*H101). P22 *pro*-3 is a specialized transducing phage carrying an insertion including *pro*A and *pro*B of *Salmonella typhimurium* (Chan, 1974; Chan & Botstein, 1976). P22 Tc-10 *tet*^{R} c2-*ts*30, P22 bp1 *tet*^{R} *Δ*[*att int*], P22 bp5 c2-*am*O8 13^{-}*am*H101 *Δ*[*att int*], and P22 *pro*-3 were obtained from D. Botstein. Other phage and bacterial strains are described in the preceding paper (Jackson *et al.*, 1978).

(b) *Bacteriophage lysates*

Lysates of P22 c1-7 (wild type carrying a clear plaque mutation), P22 bp1 *tet*^{R} *Δ*[*att int*], P22 bp5 c2 *am*O8 13^{-}*am*H101 *Δ*[*att int*], and P22 *pro*-3 were grown by infection of strain 18 as described in the preceding paper (Jackson *et al.*, 1978). P22 Tc-10 c2-*ts*30 was grown by heat induction. The lysogen 18(P22 Tc-10 *tet*^{R} c2-*ts*30) was grown in L broth at 32°C with aeration to about 3×10^{8} cells/ml. The culture was then shifted to 40°C, and vigorous aeration was continued until lysis.

(c) *Phage DNA preparations*

Unlabeled phage DNA was prepared as described in the preceding paper (Jackson *et al.*, 1978).

(d) *Preparation of P22* [^{3}H]*DNA*

P22 c1-7 was used to infect exponentially growing *S. typhimurium* LT2 strain 18 at a multiplicity of 5 phage/cell in M9 medium supplemented with 1·5% Casamino acids (Smith & Levine, 1964). At the time of infection, deoxyadenosine and [^{3}H]thymidine (20 Ci/mmol; New England Nuclear Corp., Boston, Mass.) were added to concentrations of 100 μg/ml and 10 μCi/ml, respectively. The culture was incubated at 37°C with aeration by shaking until lysis. Bacterial debris was removed by centrifugation at 9000 revs/min for 10 min in a JA20 rotor in the Beckman J21 centrifuge. The lysate was layered over a 7-ml shelf of 5·65 M-CsCl ($\rho = 1{\cdot}7$ g/cm^{3}) in a cellulose nitrate centrifuge tube and centrifuged for 2 h at 22,000 revs/min in a Beckman SW27 rotor. The phage band was removed from the top of the tube with a Pasteur pipet and added to 4·0 M-CsCl ($\rho = 1{\cdot}5$ g/cm^{3}). All CsCl solutions were prepared in 10 mM-Tris·HCl (pH 7·5). Subsequent purification of the phage particles by density gradient centrifugation and extraction of DNA with phenol were performed as described in the preceding paper (Jackson *et al.*, 1978). The specific radioactivity ofP22 DNA prepared by this procedure was 1×10^{5} to 2×10^{5} cts/min per μg DNA.

(e) *Preparation of P22 [^{32}P]DNA*

P22 c1-7 was used to infect *S. typhimurium* LT2 strain 18 in a low-phosphate medium (Botstein, 1968) to which carrier-free $H_3{}^{32}PO_4$ (New England Nuclear) was added at the time of infection to 10 μCi/ml. The resulting phage lysate was purified and DNA extracted as described above. Specific radioactivity of this DNA was approx. 3×10^5 cts/min per μg DNA.

(f) Eco*RI endonuclease cleavage*

DNA was digested with *Eco*RI as described in the preceding paper (Jackson *et al.*, 1978).

(g) *Agarose gel electrophoresis*

DNA molecules were separated by electrophoresis in cylindrical agarose gels as described in the preceding paper (Jackson *et al.*, 1978).

Slab gel electrophoresis was performed by the method of DeLeys & Jackson (1976). The electrophoresis buffer was 40 mM-Tris, 5 mM-sodium acetate, 1 mM-EDTA (adjusted to pH 8·2 with acetic acid). Agarose (Seakem) was made 0·7% (w/v) in electrophoresis buffer, liquified by heating, and poured to form 24 cm × 13 cm × 0·45 cm slab gels. Samples were made 2·5% (w/v) Ficoll 400 (Pharmacia), and run into the gel at 180 V for 2 min. The gels were then run at 30 V (20 mA) for 15 h at room temperature. Buffer was circulated between the upper and lower chambers to maintain constant pH.

The gels were stained for 45 min in ethidium bromide (1 μg/ml in water). DNA bands were visualized by the fluorescence of bound ethidium bromide upon illumination of the gel on a long-wave ultraviolet light source (C50 transilluminator, Ultraviolet Products). Gels were photographed on this light source using a Crown Graphic camera, Kodak Pan-X film, a u.v. filter (Ultraviolet Products) and either a Kodak number 25 or a number 9 Wratten gelatin filter. The Wratten number 9 filter was used to photograph gels for densitometric analysis, and a Kodak photographic step tablet (no. 1A, O.D. range 0·05 to 3·05) was included in the photograph to confirm the linear film response under these conditions.

(h) *Quantitation of DNA mass per band in agarose gel*

(i) *Radioactivity determination*

[^{3}H]DNA or [^{32}P]DNA fragments were electrophoresed in agarose gels and stained with ethidium bromide. A gel segment containing a band was cut out with a razor blade and placed in a small glass vial for scintillation counting. Samples containing [^{3}H]DNA were covered with 2 ml of Aquasol (New England Nuclear), agitated at 37°C for 18 to 24 h, and counted in a Nuclear Chicago mark II scintillation spectrometer (DeVries *et al.*, 1976). Samples containing [^{32}P]DNA were covered with 0·2 ml water, and Chèrenkov radiation was counted in the scintillation spectrometer.

(ii) *Densitometric determination*

Images of DNA bands on photographic negatives following agarose slab gel electrophoresis were traced on a Joyce–Loebl microdensitometer. Areas under the peaks on the traces were measured using a Numonics Graphics calculator.

(i) *DNA hybridization*

(i) *Isolation of P22* Eco*RI fragments*

A total of 100 μg ^{32}P or ^{3}H-labeled P22 DNA was cleaved with *Eco*RI, and fragments were separated by electrophoresis at 60 V for 14 h at 25°C in a 0·7% agarose slab gel (24 cm × 14 cm × 0·6 cm). Bands were cut from the gel, and the gel slices were extruded through a syringe with no needle, then through a 20-gauge needle and finally through a 25-gauge needle. About 15 ml of electrophoresis buffer was added, and the DNA was eluted over 14 h at 4°C. The agarose particles were pelleted by centrifugation in a Beckman 50Ti rotor at 30,000 revs/min for 2 h at 4°C. The supernatant was removed and the DNA concentrated by precipitation with ethanol. The final yield of a fragment was usually about 50%. Each fragment preparation was assayed for contamination with other fragments by mixing the labeled fragment with an *Eco*RI digest of unlabeled P22 DNA, and

separating the cleavage fragments by agarose gel electrophoresis. Each band was cut from the gels, and the amount of radioactive isotope in each slice was counted as described above.

(ii) *Hybridization*

Hybridization of [^{3}H]DNA to DNA fragments immobilized on nitrocellulose filters was performed by the method of Denhardt (1966).

A portion (0·025 pmol) of unlabeled (or ^{32}P-labeled) fragment was denatured in alkali, fixed to 13-mm Schleicher and Schuell type BA85 nitrocellulose filters and preincubated for 6 h at 65°C in 0·02% each of Ficoll 400, polyvinylpyrrolidone, and bovine albumin in 3 × SSC (SSC is 0·15 M-NaCl, 0·015 M-sodium citrate). ^{3}H-labeled DNA was denatured and fragmented by boiling for 40 min in 0·2 M-NaOH. 0·005 pmol ^{3}H-labeled denatured, broken, fragment was incubated with a DNA filter in 0·6 ml of the same solution used for the preincubation. After 44 h at 65°C, filters were removed, washed, dried and counted. Each annealing reaction was performed in triplicate. The rate of annealing is slow at the DNA concentrations used. Hybridization was measured as a function of time in control experiments using P22 DNA at the same molar concentration described above. Of the total labeled P22 DNA, 50% was bound to the filter at 44 h.

(j) *Nomenclature*

Bands appearing following agarose gel electrophoresis of *Eco*RI digests of P22 insertion and deletion mutant DNA are assigned letter designations according to the convention outlined in the preceding paper (Jackson *et al.*, 1978). By this system the same fragment forms P22 Tc-10 band ϵ and P22 bp1 band α. Bands in a mutant *Eco*RI digest which are not found in a P22 wild-type digest are assigned Greek letters in order of increasing electrophoretic mobility without regard to whether a given fragment was produced by two *Eco*RI cleavages or was derived from *Eco*RI cleavage of an end of a mature linear chromosome.

3. Results

(a) Eco*RI cleavage fragments of P22 mature chromosomes*

When circularly permuted P22 chromosomes are cleaved with restriction endonuclease *Eco*RI, and the cleavage products are separated by electrophoresis on agarose gels, eight bands are seen (Fig. 1(a)) (Helling *et al.*, 1974; Jackson *et al.*, 1978). Two of these bands, A and D, are unusual. Band A contains fragments which are heterogeneous in size, since the band is wide and diffuse. Band D is stained less intensely than the faster migrating band E, and so is present in lower molar yield than band E. It seemed likely that these unusual bands are a consequence of the limited circular permutation of P22 mature DNA, since no such anomaly is seen among the *Eco*RI cleavage products of λ DNA (Thomas & Davis, 1975).

The unusual features of the P22 *Eco*RI digest which can be seen by inspection of the gel in Figure 1(a) were studied in more detail. The lengths of fragments comprising P22 band A were measured in electron micrographs (see Jackson *et al.*, 1978). The lengths of the fragments correspond to a range of molecular weights from about 10×10^6 to 13×10^6. This result confirms the expectation that the fragments in band A are heterogeneous in size.

The molecular weights of the P22 *Eco*RI fragments have been determined and are shown in Table 1. These values were used to determine the molar yield of P22 *Eco*RI fragments. The molar yield of each band appearing after agarose gel electrophoresis was measured by three different methods. The results are shown in Table 2. Results of parallel determinations using λ *Eco*RI fragments are included for comparison. As expected, the molar yield of P22 fragment D is low; there are only about one-

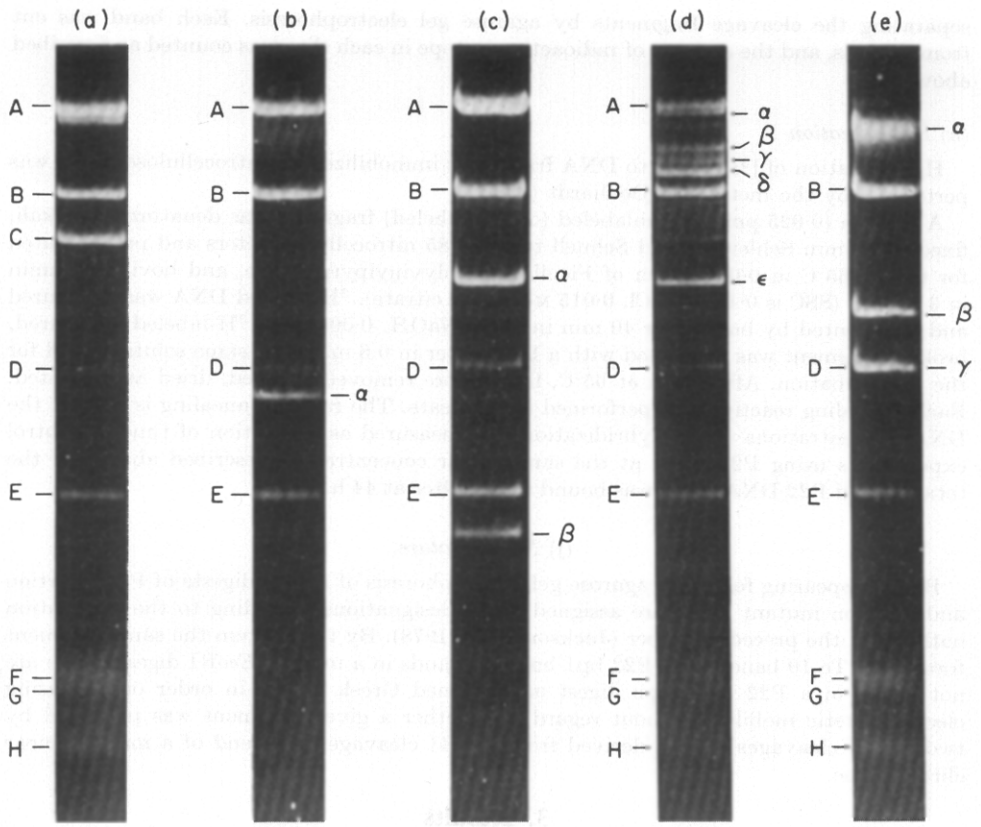

FIG. 1. Agarose gel electrophoresis of *Eco*RI digests of P22 and P22 deletion and insertion DNAs (a) P22 c1-7 DNA (wild type); (b) P22 bp5 DNA (16% net deletion); (c) P22 bp1 DNA (7% net deletion); (d) P22 Tc-10 DNA (20% insertion); (e) P22 *pro*-3 DNA (3% net insertion).

DNA was isolated from mature phage particles and cleaved to completion with endoR·*Eco*RI. Electrophoresis in 0·7% agarose gels was performed and the gels stained in ethidium bromide and photographed while illuminated with u.v. light (see Materials and Methods). P22 bands are labeled by capital letters in order of increasing electrophoretic mobility. Bands appearing as products of *Eco*RI cleavage of deletion or insertion DNAs are labeled by Greek letters.

third as many molecules of fragment D as of fragment C. In addition, the molar yields of two other fragments, A and B, are significantly less than the yield of C. Thus the P22 fragments appearing after *Eco*RI cleavage are not present in equimolar yield. In contrast, the six λ *Eco*RI fragments are present in equimolar amounts as expected (Table 2; Thomas & Davis, 1975).

(b) *Positions of molecular ends define a physical map of headful maturation events*

When a concatemer is cleaved during P22 DNA encapsulation, the products are a population of molecules whose ends fall at a variety of locations relative to restriction enzyme cleavage sites. Restriction endonuclease digestion of these different permuted molecules will generate different sets of fragments. In a population of circularly permuted DNA molecules, the nucleotide sequence between two adjacent restriction enzyme cleavage sites will sometimes be intact, and will sometimes be

TABLE 1

Molecular weights of Eco*RI cleavage fragments of P22 DNA*

P22 *Eco*RI fragment	Molecular weight ($\times 10^{-6}$)	P22 bp5 *Eco*RI fragment	Molecular weight ($\times 10^{-6}$)	P22 bp1 *Eco*RI fragment	Molecular weight ($\times 10^{-6}$)	P22 Tc-10 *Eco*RI fragment	Molecular weight ($\times 10^{-6}$)	P22 *pro*-3 *Eco*RI fragment	Molecular weight ($\times 10^{-6}$)
A	12·96†	A	12·96	A	12·96	A	12·96	α	9·4 — 10
B	6·10	B	6·10	B	6·10	α	9·7	B	6·10
C	4·77	D	2·65	α	3·73	β	7·6	β	3·18
D	2·65	α	2·40	D	2·65	γ	6·9	D + γ	2·65
E	1·59	E	1·59	E	1·59	δ	6·6	E	1·59
F	0·75			β	1·15	B	6·10	F	0·75
G	0·72					ε	3·7	G	0·72
H	0·56					D	2·65	H	0·56
						E	1·59		
						F	0·75		
						G	0·72		
						H	0·56		

† Molecular weight of intact fragment A.

Molecular weights of *Eco*RI fragments of each phage DNA are given in the order the fragments appear in the gel in Fig. 1. P22 fragments are designated by capital letters. Bands which appear in a deletion or insertion mutant but not in the P22 parent are designated by Greek letters.

The molecular weight of intact fragment A was obtained by length measurements on electron micrographs of P22 bp1 *Eco*RI A (Jackson *et al.*, 1978). Band A of P22 wild type contains smaller segments of fragment A produced by DNA packaging. Molecular weights of all other fragments were determined from measurements of electrophoretic mobilities in agarose gels as described by Jackson *et al.* (1978) in the preceding paper. The molecular weights are mean values calculated from 5 or more gels. The molecular weights determined for P22 fragments B to H in *Eco*RI digests of the deletion and insertion DNAs are in good agreement with the values determined for the same fragment in digests of P22 DNA. For simplicity, the molecular weight determined in P22 digests is given in the Table for parental fragments in mutant digests.

TABLE 2

Molar yields of λ, P22, P22 pro-*3, and P22 Tc-10* Eco*RI cleavage fragments*

λ *Eco*RI fragment	Molar yield (%) (a)	(b)	(c)	Average	P22 *Eco*RI fragment	Molar yield (%) (d)	(e)	(f)	Average
A	97	92	81	90	A	72	73	63	69
B	100	100	100	100	B	79	68	72	73
C + E	108	105	98	104	C	100	100	100	100
D	103	94	101	99	D	35	30	31	32
F	94	102	102	99	E	106	95	109	103
					F + G	88	93	104	95
					H	83	86	93	87

P22 *pro*-3 *Eco*RI fragment	Molar yield (%) (g)	(h)	Average	P22 Tc-10 *Eco*RI fragment	Headful	Molar yield (%) (i)
α	80	99	90	α	3	24
B	84	98	91	β	2	26
β	103	99	101	γ	1	32
D + γ	155	158	159	D	1	41
E	100	100	100			
F + G	105	112	109			
H	94	88	91			

P22 and λ DNAs were cleaved with *Eco*RI and fragments separated by agarose gel electrophoresis as described in Materials and Methods. The amount of DNA in each band was measured and the molar yield calculated relative to λ*Eco*RI B, P22 *Eco*RI C, P22 *pro*-3 *Eco*RI E, or P22 Tc-10 *Eco*RI E. Amount of DNA in a band was measured by 1 of 3 different methods.

(a), (d) and (h) Scintillation counting of [^{3}H]DNA.

(b) and (e) Scintillation counting of [^{32}P]DNA.

(c), (f), (g) and (i) Densitometric measurement of band image on a photographic negative.

Molar yield calculations use the molecular weights given by Thomas & Davis (1975) for λ*Eco*RI fragments and molecular weights for P22 and P22 mutant *Eco*RI fragments given in Table 1. Values in each column are mean results from 10 gels ((a) and (b)); 3 gels (c); 24 gels ((d) and (e)); 3 gels ((f), (g), (h) and (i)).

The slightly high molar yield of P22 Tc-10 *Eco*RI D is probably due to contamination with heterogeneous short segments of *Eco*RI A from the second headful and fragments of *Eco*RI δ from the fourth headful, both of which have calculated mean molecular weights similar to *Eco*RI D.

interrupted by molecular ends. If molecular ends preferentially fall in one region of the genome, some restriction fragments will be more frequently lost than others. Therefore, an *Eco*RI digest of a collection of P22 linears might contain some *Eco*RI fragments in low yield. The digest will also include a variety of fragments from the ends of linear molecules and, if enough linears have the same ends, such fragments will form visible bands in gels.

To determine precisely how molecular ends affect the bands obtained on gel electrophoresis of an *Eco*RI digest of P22 DNA, we compared these bands with those obtained from *Eco*RI digests of P22 deletion and insertion mutant DNAs. These mutations increase or decrease the genome size but do not alter headful length or the

position at which packaging begins or the direction in which sequential packaging proceeds (Tye *et al.*, 1974*a*,*b*). In such deletion or insertion mutants, the ends of mature linear DNA molecules will be at new positions relative to *Eco*RI sites. By comparing the mutant and wild-type digests we determined what bands are derived from molecular ends, and from the molecular weights of the end fragments, we placed the maturation cleavages on the *Eco*RI map of each mutant DNA. From these various maturation cleavage maps we could locate the specific site of packaging initiation and the direction of sequential packaging relative to the *Eco*RI site map. The physical map of maturation cleavages during encapsulation of wild-type P22 DNA summarizes our conclusions (Fig. 2). From the results of the preceding paper (Jackson *et al.*, 1978) we obtain the circular order of *Eco*RI fragments ...BECGFHA.... The comparisons of wild type and deletion and insertion mutant *Eco*RI digests confirm that the complete map of P22 DNA is a circular assembly of these seven fragments (Fig. 2). The specific packaging initiation site (for which we propose the new genetic term *pac*) is located in fragment A, $4{\cdot}1 \times 10^3$ base-pairs clockwise (Fig. 2) from *Eco*RI cleavage site 1. Sequential packaging proceeds in the counterclockwise direction relative to the fragment map in Figure 2. Although for any single mutant digest, alternative positions for *pac* or the reverse direction of sequential encapsulation might be congruent with the fragments observed, only the scheme of Figure 2 accounts for all the fragments seen in the four different mutant *Eco*RI digests as well as the digest of wild-type DNA. The analysis of the mutant digests is presented in detail below.

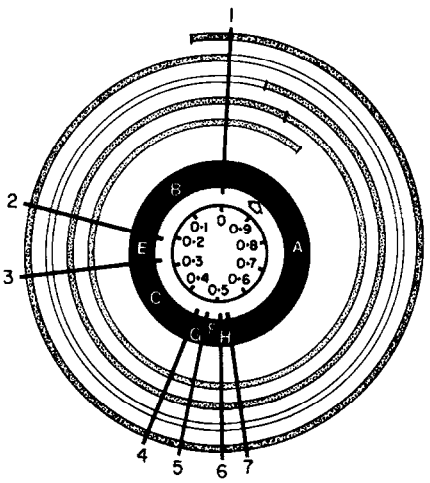

FIG. 2. Map of *Eco*RI cleavage sites and headful maturation cleavages in P22 DNA. The circular *Eco*RI cleavage map of P22 DNA is diagrammed to scale. *Eco*RI fragments are lettered. The numbered *Eco*RI cleavage sites are shown as radii of the circle. A segment of a concatemer is shown diagrammatically as a spiral wound around the circular fragment map. The concatemer may extend beyond the length in the Figure. Headful encapsulation of DNA begins at the packaging initiation site (*pac*) in fragment A shown by arrow (4100 base-pairs from *Eco*RI site 1) and sequential headfuls proceed along the concatemer in thecounterclockwise direction relative to the fragment map. In the Figure the length of one headful is 103% of the contour length of the fragment map. Positions of headful cleavage events producing mature linear molecules are to scale (polar co-ordinates). The lengths of headfuls can vary slightly (diagrams not shown). Physical map co-ordinates are shown on the inner circle. Fragment D is the short segment of *Eco*RI A in the first headful defined by *Eco*RI cleavage site 1 and *pac*.

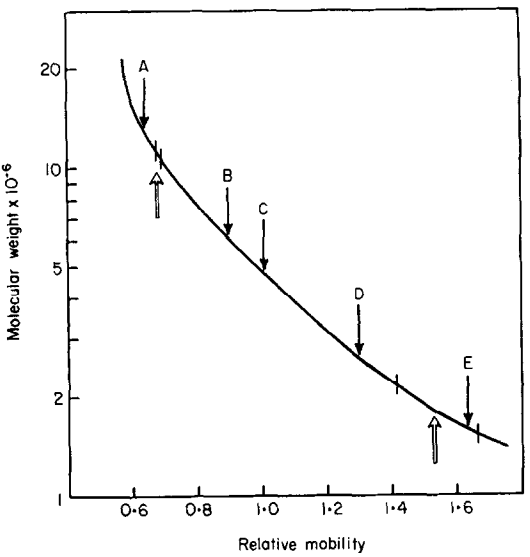

FIG. 3. Separation of fragments in an *Eco*RI digest of P22 DNA by agarose gel electrophoresis. The standard curve relating molecular weight to electrophoretic mobility in 0·7% agarose gels was obtained by measuring mobility of DNA molecules of known size under the conditions of electrophoresis defined in the preceding paper (Jackson *et al.*, 1978). Mobility of intact P22 fragments A through E are indicated above the curve by filled arrows. Molecular weights of the larger and smaller pieces of *Eco*RI A produced by the maturation cleavage between the first and second headfuls were calculated assuming 103% headful length. Their predicted relative mobilities are shown by open arrows below the curve. Vertical bars crossing the curve show the change in position for each of these segments of *Eco*RI A if headful size were 102% or 104%. A 1% variation in headful size results in a substantial change in mobility of the small piece of *Eco*RI A but only a small change in mobility of the larger piece of A for 3 resons: (1) a variation in headful size of $\pm 1\%$ of the complete P22 genome is a large proportion of the size of the shorter segment of *Eco*RI A but a much smaller fraction of the size of the larger segment of *Eco*RI A; (2) relative mobility of DNA fragments is an approximately linear function of the logarithm of the molecular weight, thus causing larger mobility changes for a unit change in molecular weight for a small fragment than for a large one; (3) the correlation between log molecular weight and relative mobility for linear DNA fragments in 0·7% agarose gels becomes steeply non-linear above a molecular weight of 6×10^6 to 7×10^6 (Helling *et al.*, 1974), so that differences in mobility due to different molecular sizes are small for large DNA fragments.

(c) Eco*RI cleavage site maps of the P22 Tc-10 insertion and its deletion derivatives*

When *Eco*RI cleavage products of deletion and insertion mutant DNAs were studied, quite different sets of bands were seen for each mutant digest (Fig. 1). In order to determine which fragments are derived from molecular ends, *Eco*RI cleavage site maps were prepared for each mutant. The physical size and genetic location of each deletion or insertion has been determined by Tye *et al.* (1974*a*). This information, together with the correlation of the *Eco*RI site map with the genetic map described in the preceding paper, facilitated mapping *Eco*RI sites on the mutant genomes. The deletion mutants bp1 and bp5 are both derived from the insertion mutant Tc-10, so the *Eco*RI cleavage site maps of these three chromosomes are related. The fourth mutant, the insertion strain P22 *pro*-3, is not related to the other three, and its *Eco*RI cleavage site map is described later.

The DNA of specialized transducing phage P22 Tc-10 contains a large ($8{\cdot}3 \times 10^3$ base-pairs) insertion of foreign DNA (Tye *et al.*, 1974*a*). The insertion includes genes which determine resistance to the antibiotic tetracycline. Since the tet^R insertion is

about 20% the length of a complete set of P22 genes, and a P22 phage head packages a headful of DNA equal in length to about 102 to 103% of one complete set of P22 genes, each particle of P22 Tc-10 contains an incomplete set of phage genes. Chan (1974) selected plaque-forming revertants of the defective P22 Tc-10. Two of these revertants, P22 bp5 and P22 bp1, were shown to carry large deletions which remove part of the tet^R insertion and some non-essential phage genes. Each of the deletions reduces the size of the genome so that a complete set of essential P22 genes can fit into one phage head. The size of each deletion exceeds the size of the tet^R insertion. Tye *et al.* (1974*a*) showed that the P22 bp1 genome, which is 95% of the length of wild type, was generated by a $10{\cdot}4 \times 10^3$ base-pair deletion of the P22 Tc-10 parent. Similarly, P22 bp5, 86% as long as wild type, was produced by a $14{\cdot}1 \times 10^3$ base-pair deletion in P22 Tc-10.

(i) Eco*RI cleavage sites in P22 bp5 DNA*

*Eco*RI cleavage products of linear P22 bp5 DNA were separated by agarose gel electrophoresis (Fig. 1(b)). The P22 bp5 digest lacks P22 *Eco*RI bands C, F, G and H. Therefore, the deletion removes P22 *Eco*RI sites 4, 5 and 6 (see Figs 2 and 4(d)). Since there is only one new fragment (α in Fig. 1(b)), no *Eco*RI site is present in the short piece of the tet^R insertion retained in P22 bp5. The new fragment α is therefore generated by cleavage at P22 *Eco*RI sites 3 and 7. The sum of the molecular weights of the P22 bp5 fragments (less fragment D) equals $23{\cdot}1 \times 10^6$, 84% of the sum of the fragments of wild-type DNA. This genome length is in good agreement with the value of 86% obtained by Tye *et al.* (1974*b*) from heteroduplex measurements. The complete *Eco*RI cleavage site map of the P22 bp5 chromosome is shown in Figure 5.

(ii) Eco*RI cleavage sites in P22 bp1 DNA*

The *Eco*RI fragments of mature P22 bp1 DNA are shown in Figure 1(c). The digest lacks P22 fragments C, F, G and H, so the deletion removes P22 *Eco*RI sites 4, 5 and 6. Two new fragments appear, so the portion of the tet^R insertion remaining in P22 bp1 bears an *Eco*RI cleavage site. Since the new fragment α is found in the P22 Tc-10 parent, but β is not (see below), the orientation of these two fragments must be that shown in Figure 4(f). The cleavage site map of P22 bp1 is given in Figure 6. The sum of the molecular weights of the P22 bp1 *Eco*RI pieces (excluding fragment D) is $25{\cdot}5 \times 10^6$, or 93% of P22 wild type. This measurement of the size of the P22 bp1 genome agrees well with the value of 95% for this mutant genome calculated from heteroduplex analysis (Tye *et al.*, 1974*a*; Chan & Botstein, 1976).

(iii) Eco*RI cleavage sites in P22 Tc-10 DNA*

P22 Tc-10, which carries the tet^R insertion, has no deletion of P22 sequences (Tye *et al.*, 1974*b*). Therefore the insertion will cause only one wild-type *Eco*RI fragment to be missing from the Tc-10 *Eco*RI digest. Figure 1(d) shows that P22 *Eco*RI fragment C is the only fragment missing from the digest. The tet^R element is therefore inserted in fragment C between P22 *Eco*RI sites 3 and 4 in P22 Tc-10.

The P22 Tc-10 digest also contains a number of new bands not produced by *Eco*RI cleavage of wild-type P22. P22 Tc-10 band ϵ is identical to band α of P22 bp1 and therefore is derived from *Eco*RI cleavage at P22 site 3 and an *Eco*RI site in the tet^R insertion. Band δ is produced by cleavage at the *Eco*RI site in the tet^R

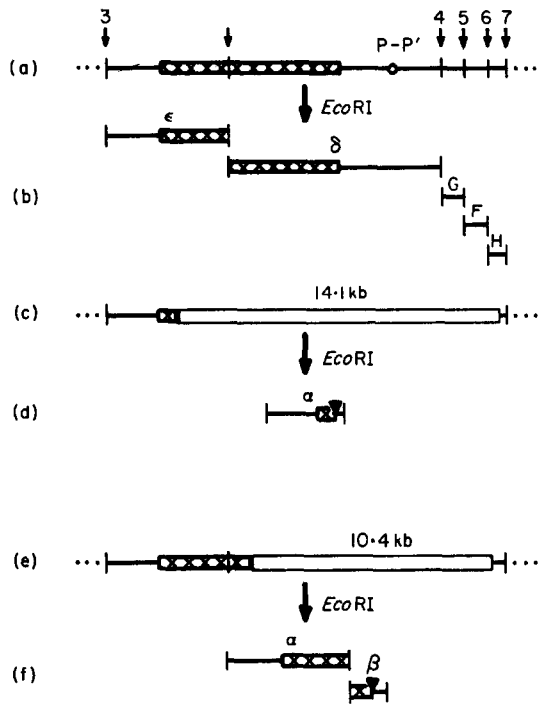

FIG. 4. *Eco*RI cleavage site maps of the Tc-10 *tet*^{R} insertion and the bp1 and bp5 deletions between P22 *Eco*RI sites 3 and 7.

Positions of *Eco*RI cleavage sites (Jackson *et al.*, 1978) are to scale. Cleavage site numbers correspond to the P22 wild-type cleavage map (Fig. 2). kb, 1000 bases.

(a) Physical gene map to scale of P22 Tc-10 DNA between P22 *Eco*RI cleavage sites 3 and 7. Size of DNA segment shown is $18{\cdot}7 \times 10^3$ bases. Physical co-ordinates of the phage attachment site (○) relative to the *tet*^{R} insertion from the data of Chan & Botstein (1976). (X X X X) Indicates the *tet*^{R} insertion. Size of the insertion is 20% of the size of the complete P22 genome. P-P′ is located $2{\cdot}5 \times 10^3$ bases from the right end of the *tet*^{R} insertion and $13{\cdot}5 \times 10^3$ bases from *Eco*RI site 3. Gene *int* is to the right of P-P′ but left of site 7, and gene *erf* is to the right of site 6.

(b) P22 Tc-10 *Eco*RI fragments derived from the region of the chromosome diagrammed in (a).

(c) Physical gene map of P22 bp5 DNA between P22 *Eco*RI cleavage sites 3 and 7. The open bar represents the deletion. Size of the deletion is calculated from the data in Table 2.

(d) P22 bp5 *Eco*RI fragment derived from the region of the chromosome diagrammed in (c). (▼) Represents the site of the deletion.

(e) Physical gene map of P22 bp1 DNA between P22 *Eco*RI cleavage sites 3 and 7. The open bar represents the deletion. Size of the deletion is calculated from the data in Table 2.

(f) P22 bp1 *Eco*RI fragments derived from the region of the chromosome diagrammed in (e). P22 bp1 fragment α is the same as Tc-10 fragment ε.

insertion and at P22 *Eco*RI site 4 (Fig. 4(a) and (b)). The sum of the molecular weights of the two fragments δ and ε is $10{\cdot}3 \times 10^6$ (Table 1), in good agreement with the value $10{\cdot}5 \times 10^6$ expected from a 20% insertion in fragment C. The other new P22 Tc-10 bands α, β and γ are a consequence of headful packaging of the oversize Tc-10 DNA (see below). Therefore Tc-10 contains one more *Eco*RI cleavage site than wild type. This additional *Eco*RI site is located in the *tet*^{R} insertion which occurred in P22 fragment C (Figs 4(a) and 7).

(d) *The* pac *site lies in* Eco*RI fragment A*

In the *Eco*RI digests of Tc-10, bp1 and bp5 mutant DNAs, band A is sharp and band D is present in low yield (Fig. 1 (b) to (d)). These results led us to propose that

both fragment D and the heterogeneous smaller fragments in band A of a wild-type digest are produced by *Eco*RI cleavage near ends of linear molecules. Since the only molecular end which falls at the same position on wild type and mutant genomes is the end of the first chromosome encapsulated at *pac*, we postulated that *Eco*RI cleavage of the first DNA headful of all these phages produces fragment D. Therefore *pac* would be located $4{\cdot}1 \times 10^3$ bases (the length of fragment D) from an *Eco*RI cleavage site. All other molecular ends will be at different positions in each mutant compared to wild type. Since all three mutants have only one size of fragment in band A, we conclude that in wild type the heterogeneous smaller fragments are produced by *Eco*RI cleavage of linear molecules having ends at varying positions within fragment A (see Fig. 2). In the Tc-10 insertion phage and the bp1 and bp5 deletion mutants, the size of the genome has increased or decreased while the length of a headful is unchanged, so that ends of mature linear molecules no longer fall primarily in fragment A (see Figs 5 to 7). The position of wild-type permuted ends in each sequential headful moves only 3% along the genome, and so these ends fall in the vicinity of *pac*. Therefore, the proposal that permuted ends of wild-type molecules fall primarily in *Eco*RI A suggests that *pac* should also lie in fragment A.

The proposal that fragment D is a subset of the nucleotide sequences of P22 *Eco*RI A was tested directly by measuring hybridization between fragment D and each of the other P22 *Eco*RI fragments. Fragment D hybridizes to fragment A but not to any of the other P22 *Eco*RI fragments (Table 3). Fragment D is therefore identical to a nucleotide sequence contained in fragment A, and this sequence is found in no other region of the P22 genome.

Since fragment D is a segment of fragment A, *pac* should be between *Eco*RI sites 1 and 7, and within $4{\cdot}1 \times 10^3$ bases (10% of the P22 genome) of one of the sites. The

TABLE 3

Hybridization between Eco*RI fragments of P22 DNA*

DNA on filter		[^{3}H]DNA in solution		Hybridization (%)	
P22 *Eco*RI fragment	μg	P22 *Eco*RI fragment	μg	(a)	(b)
A	0·32	A	0·064	52	54
A	0·32	D	0·013	50	52
A	0·32	E	0·008	7	7
E	0·04	D	0·013	14	15

The *Eco*RI cleavage fragments used were prepared from P22 wild-type DNA. Specific activity of the [^{3}H]DNA is $1{\cdot}0 \times 10^5$ cts/min per μg. A total of 0·025 pmol of a fragment was fixed to a filter and incubated with 0·005 pmol ^{3}H-labeled fragments in solution. Blank filters included in each hybridization vial bound 0·5% of the total ^{3}H-labeled DNA. Percentage hybridization is the ratio of the ^{3}H-labeled DNA hybridized to the total ^{3}H-labeled DNA. The values given are the average of 3 annealing reactions performed in parallel, and (a) and (b) are results of 2 independent hybridization experiments.

The *Eco*RI A preparation fixed to the filter contains 2% (0·006 μg) *Eco*RI E, and the *Eco*RI E preparation bound to the filter contains 3% (0·001 μg) *Eco*RI D. In addition, 5% by weight of the [^{3}H]*Eco*RI D preparation is *Eco*RI E. Therefore, the apparent low level of annealing of [^{3}H]E to A, or [^{3}H]D to E is due to hybridization of contaminating fragments. When each of the P22 *Eco*RI fragments A, B, C and E was annealed with the same fragment on the filter, about 50% of the input [^{3}H]DNA hybridized to the filter. When *Eco*RI [^{3}H]D preparations were incubated with each of these fragments fixed to filters, 15% or less of the ^{3}H-labeled DNA bound to the filter (data not shown for all fragments).

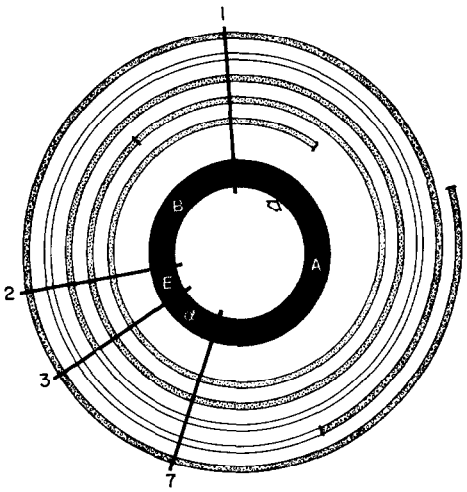

FIG. 5. Map of *Eco*RI cleavage sites and headful maturation cleavages in P22 bp5 DNA.
The circular *Eco*RI cleavage map of P22 bp5 DNA is diagrammed to scale. The P22 bp5 genome is 84% the size of P22 wild-type (Fig. 2). Symbols are as in Fig. 2. The model for P22 DNA maturation described in Fig. 2. was used to predict the positions of headful cleavages shown.

fact that band B is found in low yield in the wild-type digest suggests that some ends of wild-type linears fall within B and therefore that *pac* is nearer *Eco*RI site 1, and that sequential packaging proceeds in the counterclockwise direction (Fig. 2). The placement of fragment D at the *Eco*RI site 1 end of fragment A is further supported by the results of *Sma*I restriction enzyme digestion of P22 DNA. *Sma*I cleaves P22 DNA twice. Both sites are located at the *Eco*RI site 1 end of fragment A at map co-ordinates 0·91 and 0·87 (R. J. Deans, unpublished experiments). Fragment D is cleaved once by *Sma*I, demonstrating that fragment D lies between *Eco*RI site 1 and co-ordinate 0·90 and includes the *Sma*I site at 0·91 on the P22 physical map. Additional evidence to support the physical map of maturation events shown in Figure 2 comes from further study of *Eco*RI digests of the insertion and deletion derivatives of P22 DNA.

(e) *Physical map of molecular ends of P22 bp5 DNA*

The consequences of headful packaging of P22 bp5 DNA in accordance with the scheme outlined above are diagrammed in Figure 5. Packaging begins at *pac*, as in wild-type DNA (Tye *et al.*, 1974*b*), and proceeds sequentially without further site specificity in the counterclockwise direction. The size of the DNA headful cleaved from the concatemer is the same as in the case of wild-type phage (102 to 103% of one complete set of wild-type P22 genes). Figure 5 shows the calculated positions of headful cleavages of the P22 bp5 concatemer relative to *Eco*RI cleavage sites. *Eco*RI digestion of these P22 bp5 linear DNA molecules will produce fragment D in low molar yield as in wild type, since the site on the concatemer at which headful packaging initiates is not altered by the deletion. The diagram further shows that, in contrast to wild-type P22, fragment A is intact in early headfuls. The result of electrophoretic analysis of the *Eco*RI cleavage products of P22 bp5 is shown in Figure 1(b). Fragment D is found in low molar yield; band A is sharp and lacks the diffuse leading edge seen in *Eco*RI digests of P22 wild-type DNA. The diagram shows that third and

fourth headfuls would yield medium-sized fragments of A, and a diffuse band is present in the region of the gel (between bands A and B) where these fragments should migrate. Fragments produced by *Eco*RI cleavage of linear molecules with ends falling between *Eco*RI sites 1 and 2 are not seen. The absence of these short fragments can be explained if the length of DNA in a headful varies slightly. If this small variation is large with respect to the size of the fragment derived from a molecular end, the molecular weight distribution of the fragment would be heterogeneous and it would not form a visible band in gels. Figure 3 presents a detailed analysis of this point. Chan (1974) has independently proposed that P22 headful lengths are variable.

(f) *Physical map of molecular ends of P22 bpl DNA*

The physical location of maturation cleavages of P22 bpl DNA was calculated from the postulates outlined above, and the results are shown diagrammatically in Figure 6. An *Eco*RI digest of the resulting linear DNA molecules would contain fragment D in low molar yield, since the specificity of initiation of a packaging sequence is unchanged. Molecular ends do not fall in fragment A, so heterogeneous shorter segments of A should not appear in the digest. The fragments generated by *Eco*RI digestion of P22 bpl linear DNA support the model (Fig. 1(c)). Fragment D is found in low molar yield and band A lacks the diffuse leading edge seen in wild type. The fragments of the mature linear chromosomes corresponding to segments of *Eco*RI fragment B will vary in size due to variation in the length of the headful packaged. Since these fragments are small, the small variation in headful size will be a large fraction of their length and consequently they will not appear as visible bands. The direction of sequential packaging must be counterclockwise as shown in Figure 6, since if packaging of bpl DNA began at the site indicated but proceeded sequentially in the clockwise direction, no intact fragment A would be found.

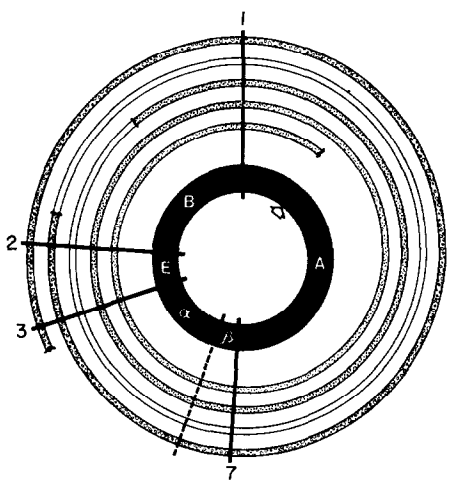

FIG. 6. Map of *Eco*RI cleavage sites and headful maturation cleavages in P22 bpl DNA. The circular *Eco*RI cleavage map of P22 bpl DNA is diagrammed to scale. The P22 bpl genome is 93% the size of P22 wild-type (Fig. 2). Symbols are as in Fig. 2. (-----) Designates the *Eco*RI cleavage site in the remaining portion of the *tet*^{R} insertion (see Fig. 4). The model for DNA maturation described in Fig. 2 was used to predict the positions of molecular ends relative to the *Eco*RI cleavage site map.

(g) *Physical location of molecular ends of P22 Tc-10 DNA*

The headful packaging scheme applied to P22 Tc-10 predicts a complex set of bands following electrophoretic separation of *Eco*RI cleavage fragments (Fig. 7). Since packaging initiates at the normal site in fragment A, the ends of the chromosomes packaged in first headfuls will yield fragment D on *Eco*RI cleavage. The first headful DNA molecule also produces a long piece of A. The second headful yields another long section of A, while one end of the third headful is a piece of A only slightly shorter than intact P22 fragment A. All these three segments of A will appear as visible bands on agarose gels despite variation in headful length, since all these fragments are over about $M_r = 7 \times 10^6$ in length (see Fig. 3 for detailed explanation).

These predictions are confirmed in Figure 1(d). Fragment D is present in low yield. Three new bands containing fragments smaller than *Eco*RI A but larger than any other *Eco*RI fragment appear. Band γ is derived from one end of the first headful, β from the second headful, and α from the third sequential headful. The molecular weights of these three fragments calculated from the diagram approximate those estimated from the mobility of the fragments in the gel (see Table 1 and the legend to Fig. 7). Intact fragment A is found in low yield, since it derives only from the fourth sequential headful in a packaging sequence.

(h) *Positions of ends of linear DNA molecules relative to* Eco*RI sites in P22* pro*-3 DNA*

An insertion mutant of P22 not derived from P22 Tc-10 also provides strong support for the packaging model of Figure 2. P22 *pro*-3 is a defective specialized

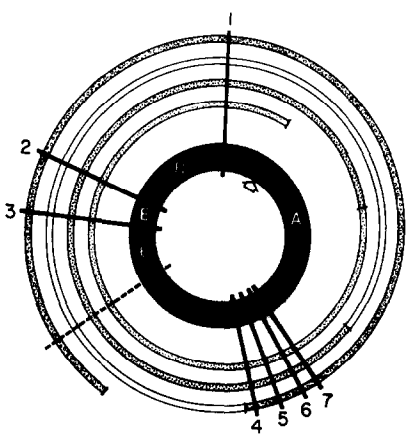

FIG. 7. Map of *Eco*RI cleavage sites and headful maturation cleavages in P22 Tc-10 DNA. The circular *Eco*RI cleavage map of P22 Tc-10 DNA is diagrammed to scale. The P22 Tc-10 genome including the tet^R insertion is 120% the size of P22 wild-type (Fig. 2). Symbols are as in Fig. 2. (------) Designates the *Eco*RI cleavage site in the tet^R insertion (see Fig. 4). The model for P22 DNA maturation described in Fig. 2 was used to predict the positions of molecular ends on the physical map of *Eco*RI cleavage sites. If the ends of linear molecules were as shown, *Eco*RI digestion of DNA packaged in the first headful would generate fragments D and γ (predicted $M_r = 6{\cdot}1 \times 10^6$) in low yield; the second headful would produce fragment β (predicted $M_r = 6{\cdot}9 \times 10^6$), the third would yield fragment α (predicted $M_r = 11{\cdot}1 \times 10^6$), and only the linear DNA molecules from the fourth sequential headful would yield intact fragment A.

transducing phage which arose by abnormal excision of a P22 prophage. This excision event generated a 6% insertion of bacterial genes and a 3% deletion of phage sequences, including part of the phage attachment site (Chan, 1974; Chan & Botstein, 1976; Jessop, 1976). The formation of P22 *pro*-3 is therefore analogous to formation of *λgal* specialized transducing phages (Chan & Botstein, 1976). Since we have shown (Fig. 4) that the prophage attachment site is located in P22 *Eco*RI C, the insertion in P22 *pro*-3 must occur between *Eco*RI sites 3 and 4. From this information, the *Eco*RI cleavage map of P22 *pro*-3 DNA shown in Figure 8 was derived. If the *pro*-3

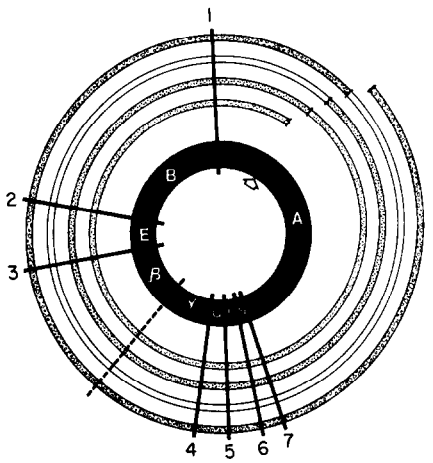

FIG. 8. Map of *Eco*RI cleavage sites and headful maturation cleavages in P22 *pro*-3 DNA. The circular *Eco*RI cleavage site map of P22 *pro*-3 DNA is diagrammed to scale. The P22 *pro*-3 genome is 103 to 104% of the size of P22 wild-type (Fig. 2). Symbols are as in Fig. 2. (– – – – –) Designates the *Eco*RI cleavage site in the *pro*-3 insertion. The model for P22 DNA maturation described in Fig. 2 was used to predict the positions of molecular ends on the physical map. The average length of a headful, 103% of the P22 wild-type genome, was used to calculate the positions of DNA maturation cleavages shown. Since the genome of the P22 *pro*-3 insertion mutant is about the same length or very slightly longer than the average length of a headful of DNA, all maturation cleavages occur near the *pac* site, and none of the mature linear chromosomes yield intact fragment A upon *Eco*RI cleavage.

insertion carries no *Eco*RI cleavage site, P22 *Eco*RI C will be replaced by a fragment equal to the molecular weight of P22 *Eco*RI C plus 3% of intact P22 DNA, or $5{\cdot}6 \times 10^6$. However, agarose gel electrophoresis of an *Eco*RI digest of P22 *pro*-3 DNA (Fig. 1(e)) showed that no fragment C was present. Instead, a single new fragment (β) of molecular weight $3{\cdot}18 \times 10^6$ was seen. However, measurement of the amount of DNA in each band showed that the molar yield of band D is 155% compared to band E (Table 2(g)). Therefore, *Eco*RI cleavage at a site within the *pro*-3 insertion yields two new fragments, fragment β, and fragment γ of molecular weight $2{\cdot}65 \times 10^6$, which co-migrates with fragment D during gel electrophoresis. The net size of the insertion calculated from the sum of the molecular weights of the two new fragments is 3·7% of the mature P22 chromosome, in good agreement with the value of 3% obtained from heteroduplex measurements by Chan & Botstein (Chan, 1974; Chan & Botstein, 1976). The order of the fragments β and γ shown on the map in Figure 8 was obtained by comparing products of *Hin*dIII and *Eco*RI digestion of P22 *pro*-3

DNA with double digestion products of P22 wild-type DNA (R. J. Deans, unpublished experiments).

The packaging model applied to P22 *pro*-3 predicted a striking alteration in P22 *Eco*RI cleavage products. The insertion results in a complete genome length nearly equal to the length of one headful. Therefore the ends of linear molecules encapsulated in sequential headfuls will all be close to the *pac* site at which encapsulation begins. The packaging model of Figure 2 is applied to P22 *pro*-3 in Figure 8. If packaging begins within *Eco*RI A at the site shown in the Figure, and one complete genome is about the same size or slightly larger than the average length of one headful, the ends of all the mature linears lie in *Eco*RI A near the *pac* site. The diagram predicts that no intact fragment A will be found. The products of *Eco*RI cleavage of P22 *pro*-3 are shown in Figure 1(e). There is no intact fragment A in the digest. This result shows conclusively that *pac* is located in A. Segments of fragment A are found which have heterogeneous molecular weights between $9{\cdot}4\times10^6$ and $10{\cdot}0\times10^6$. This result positions *pac* within $4{\cdot}5\times10^3$ bases of one end of *Eco*RI A. This result is in excellent agreement with the proposal that *pac* is $4{\cdot}1\times10^6$ bases from *Eco*RI site 1.

(i) *Physical locations of P22 genes*

The *Eco*RI cleavage site maps of the deletion and insertion mutants used to analyze DNA packaging also allow some P22 genes to be positioned relative to P22 *Eco*RI cleavage sites. Chan & Botstein prepared a physical map of a portion of the P22 genome near the prophage attachment site from genetic and heteroduplex analysis of Tc-10 and its deletion revertants (Chan, 1974; Chan & Botstein, 1976). These studies precisely located the phage attachment site relative to the tet^R insertion. This physical map is correlated with the *Eco*RI cleavage site maps of the insertion and deletion DNAs in Figure 4. We show that the right end of the bp5 deletion lies between P22 *Eco*RI sites 6 and 7. The size of the net deletion equals 16% the length of the wild-type P22 genome. Chan & Botstein showed that a piece of the tet^R insertion equal to 2% of P22 remains in bp5. This determination of the left-hand end of the deletion and the total size of the deletion places the end of the tet^R insertion with respect to *Eco*RI cleavage site 3 as shown in Figure 4(a). The prophage attachment site is $2{\cdot}5\times10^3$ bases from tet^R (Chan, 1974), and lies between *Eco*RI sites 3 and 4, at 0·4 on the physical gene map in the preceding paper (Jackson *et al.*, 1978). *int* lies to the right of the attachment site, but under the bp5 and bp1 deletions, so it is located to the right of *Eco*RI site 3 and left of *Eco*RI site 7 (Fig. 4(a)). We have not determined whether *int* is located on *Eco*RI fragments C, G or F. Gene *erf* is not deleted in bp5, so it is located to the right of *Eco*RI site 6 (Fig. 4(a)). *erf* must lie in either fragment H or A.

4. Discussion

(a) *Location of DNA packaging initiation site and direction of sequential encapsulations on the* Eco*RI cleavage site map of P22 DNA*

The *Eco*RI cleavage site map derived in this and the preceding paper (Jackson *et al.*, 1978) is the first restriction endonuclease cleavage site map of a circularly permuted chromosome. Restriction enzyme cleavage of a random set of circularly permuted chromosomes should yield as visible bands on electrophoresis only the fragments generated by restriction endonuclease cleavages at both ends of the fragment. Many other fragments would result from one endonucleolytic cleavage

near a molecular end, but if the ends were randomly distributed over the genome, these fragments would not form detectable bands. However, the P22 circular permutations are not random. The ends of the mature chromosomes fall over a limited portion of the physical map (Tye *et al.*, 1974*b*). In this case, many linear molecules have approximately the same ends, and restriction enzyme cleavage generates enough fragments of similar size to form visible bands on agarose gel electrophoresis. These end fragments were used to map the location of molecular ends relative to the *Eco*RI site map, which in turn has been oriented relative to the genetic map (Jackson *et al.*, 1978). Molecular ends fall at different positions in deletion or insertion mutant DNA, and end fragments from *Eco*RI digests of these DNAs allowed more maturation cleavage events to be mapped relative to *Eco*RI sites. From these physical locations for maturation cleavages and the known length of a headful, the position of the *pac* site and the direction of sequential packaging relative to the *Eco*RI cleavage site map could be deduced. P22 DNA maturation begins $4{\cdot}1 \times 10^3$ bases clockwise from *Eco*RI site 1 and proceeds in the counterclockwise direction in Figure 2. Fragment D is produced by *Eco*RI cleavage at site 1 near the end of a linear DNA molecule encapsulated starting at *pac*, or the first headful of DNA in a packaging sequence. One end of fragment D marks the location of *pac* within *Eco*RI fragment A. Ends of P22 wild-type linear chromosomes cleaved non-specifically during sequential packaging also fall in *Eco*RI fragment A, so that A is found in low yield, and slightly shorter segments of A are found as the leading edge of band A following gel electrophoresis. Since no short pieces of fragment A smaller than fragment D are found, although they should be produced from *Eco*RI cleavage of DNA packaged in the second and third headfuls, we suggest that the headful length varies slightly. The small variation in headful size is nevertheless a large proportion of the total size of these short fragments, leading to sufficient heterogenity in length that they are not observed as bands in gels (see Fig. 3). That the headful length should vary slightly is not surprising, and genetic experiments reported by Chan (1974) support this suggestion. Fragment D, however, is of invariant size, since it arises from two site-specific cleavages, one at *pac*, and one at *Eco*RI site 1. Since D is an end fragment and a segment of *Eco*RI A, the other seven *Eco*RI fragments ordered in the preceding paper define the positions of all *Eco*RI cleavage sites in P22 DNA. The sum of the molecular weights of these seven fragments (A, B, C, E, F, G and H) is $27{\cdot}5 \times 10^6$, in excellent agreement with the value of $27{\cdot}65 \times 10^6$ for the molecular weight of intact P22 less the 3% terminal redundancy (Rhoades *et al.*, 1968; Tye *et al.*, 1974; Jackson *et al.*, 1978). This *Eco*RI cleavage site map is a circle, since P22 linear chromosomes are circularly permuted.

Tye *et al.* (1974*b*), following another experimental approach, first proposed that P22 DNA encapsulation begins at a unique genetic site and proceeds sequentially in one direction. Our results are additional evidence for this model of P22 DNA packaging. These experiments furthermore locate the specific site at which P22 DNA maturation begins, and the direction of sequential encapsulation relative to the *Eco*RI cleavage site map of P22 DNA.

(b) Eco*RI analysis of P22 DNA packaging*

Analysis of *Eco*RI cleavage products of P22 DNA provides a sensitive and simple means to study P22 headful packaging. Measurements of the relative yields of

fragments derived from ends of linear molecules can be used to determine the proportion of linears packaged in first or subsequent headfuls. Since fragment D comes only from chromosomes packaged at *pac*, the relative molar yield of D represents the fraction of linear chromosomes produced by the initial headful in a packaging sequence. Therefore, about one-third of the wild-type P22 linear chromosomes encapsulated are first headfuls (Table 2).

Electrophoresis of the P22 Tc-10 *Eco*RI digest yields bands uniquely characteristic of the first, second and third headfuls in a packaging sequence (Figs 1(d) and 7). P22 Tc-10 bands D and γ are products of *Eco*RI cleavage of a first headful, band β is produced only by cleavage of a second sequential headful, and band α comes only from cleavage of a linear packaged in a third sequential headful. The molar yield of each of bands γ, β and α equals the proportion of linear chromosomes encapsulated in first, second or third headfuls. The molar yield data for band γ in Table 2 show that about one-third of the linear chromosomes were packaged in initial headfuls. About one-quarter of the linears were packaged in a second headful (band β) or a third sequential headful (band α). There is no band which uniquely distinguishes a fourth headful, but these results show that over 80% of the mature linear chromosomes were packaged in the first three sequential headfuls (Table 2). We expect that most packaging sequences do no extend beyond four headfuls. These results do not conflict with the data from which Tye *et al.* (1974*b*) concluded that the maximum number of headfuls in one sequence is ten. They showed that the ends of linear molecules are distributed over 20% of the physical map, and most ends fall within 10 to 15% of each other (Tye *et al.*, 1974*b*). We have used the value of 103% for the length of one average headful, since calculations based on this figure give the best fit with the molecular weights of *Eco*RI fragments observed in P22 Tc-10 (Fig. 7). This value implies a terminal redundancy of 3%, which falls within the range of lengths of terminal redundancies measured previously (Tye *et al.*, 1974*a*). If the length of an average headful is 103% of one complete set of P22 genes, and if there are four headfuls in one sequence, the ends of linear molecules will fall over 12% of the physical map. Variability in headful size will cause the ends to be distributed over a slightly larger portion of the map, in good agreement with the previous data showing the distribution of molecular ends (Tye *et al.*, 1974*b*).

The accompanying paper (Weaver & Levine, 1978) further illustrates the utility of *Eco*RI cleavage for study of P22 DNA packaging. They have analyzed *Eco*RI digests of the mixture of host and phage DNA obtained from defective particles produced following induction of a P22 prophage unable to excise from the host chromosome. The subset of P22 *Eco*RI fragments found indicates that the initiation site and direction of DNA packaging in this abnormal case is the same as in wild-type P22.

(c) *Genetic location of the packaging initiation site*

The physical map of *Eco*RI cleavage sites in P22 DNA (Fig. 2) has been aligned with the P22 genetic map, and a number of P22 genes have been precisely located with respect to *Eco*RI cleavage sites (see Fig. 6 of Jackson *et al.*, 1978). This physical gene map allows us to relate the physical map of packaging events (Fig. 2) to the genetic map. Packaging begins on the late gene side of gene *13*, and moves in the counterclockwise direction with respect to the genetic map given in Figure 6 by Jackson *et al.* (1978), or away from the early gene region. Weaver & Levine (1978) have also

concluded that encapsulation of a P22 prophage unable to excise from the host chromosome is polarized in this same direction.

A fundamental question about the molecular basis of P22 DNA packaging concerns the nature of the interaction between P22 proheads and the packaging initiation site on the concatemeric DNA precursor (Tye *et al.*, 1974*b*; Tye, 1976). The nucleotide sequence corresponding to this site occurs in each monomeric repeating unit of the concatemer. Yet a packaging sequence begins only once per three or four genome repeats. Tye *et al.* (1974*b*) suggested that the unique site at which encapsulation begins is a free end of the concatemeric DNA at the tail of a rolling circle. Thus the unique genetic site for phage DNA encapsulation would be located at the site of origin of P22 DNA synthesis. Our data now exclude this interpretation. The only known site for initiation of P22 DNA replication lies in the vicinity of DNA synthesis genes *12* and *18* (Hilliker & Botstein, 1976). Genes *12* and *18* can be placed in fragment A at a maximum distance of 11×10^3 bases from P22 *Eco*RI cleavage site 7 from consideration of *λimm*P22hy37 (Jackson *et al.*, 1978). The site of packaging initiation is $15{\cdot}9 \times 10^3$ bases from site 7 (Fig. 2). The physical map shows unequivocally that the packaging initiation site is not located at genes *12* and *18*, and therefore is unlikely to be a free end produced by DNA replication. Weaver & Levine (1978) concluded that during induction of a P22 *int*$^-$ lysogen, all regions of the P22 genome are replicated, although only part of the prophage sequences are encapsulated. This result is additional evidence that DNA replication is not the sole determinant of encapsulation specificity.

All available data suggest that the *pac* site is near gene *3*. Since *λimm*P22hy38 includes P22 gene *13* within less than 15×10^3 bases of DNA from site 7 (in counterclockwise direction in Fig. 2) (Jackson *et al.*, 1978), and the packaging origin is $15{\cdot}9 \times 10^3$ bases counterclockwise from site 7, the site at which headful packaging begins lies beyond gene *13*. These results are in agreement with approximate locations for the packaging initiation site obtained by genetic methods which place the site within the following genetic region: genes *18 12 13 19 3 2*. Analysis of the plating efficiency of P22 *pro*-3 on various P22 deletion lysogens led Chan to suggest that the packaging origin lies at one or the other end of the region encompassing genes *12* through *3* (Chan, 1974). From study of excision-defective P22 lysogens, Weaver & Levine (1978) conclude that this site is to the left of gene *2* in the gene order given above, and they suggest that the site may be in or near gene *3*. We have shown that it is to the right of gene *13*. These various lines of evidence taken together indicate that the packaging initiation site lies in the vicinity of genes *19* and *3*.

(d) *P22 DNA encapsulation and maturation may resemble the λ mechanisms*

Although the organization of genes in the early region of the λ and P22 genetic maps are similar, the mature form of the chromosomes of the two viruses are quite different. P22 linear DNA molecules have circularly permuted ends, while λ chromosomes have unique ends. Since the final form of a mature phage chromosome is a consequence of the mechanism by which DNA is cut from the concatemer, the mechanisms by which P22 and λ process DNA during encapsulation were thought to be fundamentally different (Tye, 1976; Botstein *et al.*, 1972; Feiss & Bublitz, 1975). However, our results, when considered together with recent work on λ DNA maturation, show that P22 and λ DNA maturation mechanisms have many common properties.

The product of P22 gene *3* may be directly involved in cutting the concatemer at the packaging initiation site (Botstein *et al.*, 1973; Tye, 1976; Raj *et al.*, 1974). The position of gene *3* on the P22 genetic map is analogous to the genetic location of λ gene *A*, which is thought to specify the nuclease which cleaves λ concatemers during λ maturation (Botstein *et al.*, 1972; Wang & Kaiser, 1973). Both P22 gene *3* and λ gene *A* map adjacent to lysis genes at one end of the clustered head genes. We favor the proposal that interaction of the product of gene *3* at *pac* is required to begin a sequence of headfuls at the packaging initiation site. Gene *3* product may have endonucleolytic activity, or may control the activity of another nuclease (Tye, 1976; Botstein *et al.*, 1973; Raj *et al.*, 1974).

The P22 packaging initation site has been located in a region on the P22 chromosome including genes *19* and *3* (see above; Chan, 1974; Weaver & Levine, 1978). The λ *cos* site, at which the λ site-specific nuclease acts to cut the concatemeric DNA precursor, lies between lysis genes and head genes adjacent to gene *A*, a region of the λ map analogous to the region between P22 genes *19* and *3*. The physical location of the P22 packaging initiation site corresponds to λ *cos* as well. When the physical–genetic map of a P22 chromosome which was encapsulated at the packaging initiation site is aligned at the prophage attachment site with the physical gene map of λ, the ends of the right arms which mark the physical locations of *pac* and *cos* are closely aligned (see Fig. 7 of the preceding paper, Jackson *et al.*, 1978). Thus the physical and genetic map locations of the genes which specify or control a DNA maturation nuclease and the specific site of action of the nuclease are similar in P22 and λ.

Headful packaging of sequential headfuls of P22 DNA proceeds in one direction along a concatemer (Tye *et al.*, 1974*b*). The direction of packaging is away from early genes and lysis genes, or counterclockwise (Fig. 2). λ chromosomes also are packaged and cut from a concatemer sequentially, with the last cut made in packaging one chromosome serving as the first cut in maturation of the next (Emmons, 1974; Feiss & Bublitz, 1975). The processive packaging and cutting of λ DNA occurs in only one direction along the concatemer. λ processive packaging is polarized in the same direction relative to the genetic map as P22 sequential packaging (Feiss & Bublitz, 1975; Sternberg & Weisberg, 1975). The number of λ chromosomes packaged in a sequence is two to three (Emmons, 1974; Feiss & Bublitz, 1975), while three to four P22 headfuls are encapsulated sequentially (Table 2).

(e) *Initiation of a packaging sequence*

What limits the length of a packaging sequence? λ DNA concatemers ten times the length of mature λ DNA have been reported (Skalka, 1971). Emmons (1974) proposed that a λ packaging sequence can initiate at any *cos* site on a concatemer. Feiss & Bublitz (1975) suggest that several packaging sequences are initiated at random on one concatemer. P22 DNA concatemers ten genomes long have been reported in the absence of head assembly and DNA processing (Botstein, 1968; Botstein & Levine, 1968; Botstein *et al.*, 1973). We show here that most P22 packaging sequences comprise three to four headfuls. These data suggest that P22 can initiate several packaging sequences on one concatemer, and the length of a packaging sequence reflects the probability that gene *3* product will interact with a *pac* site. We offer two suggestions to explain why only one in every three *pac* sites on a concatemer is cleaved. Perhaps gene *3* product competes with encapsidation for free *pac* sites. Alternatively, gene *3* product might be made in low amounts and would act non-

catalytically. In this case, *pac* sites would be in excess over specific nucleolytic activity, and only one in three sites could be cleaved. Previous workers suggested that P22 initiates a headful packaging sequence once per concatemer at a free end of DNA which might be the tail of a rolling circle DNA replication intermediate (Tye *et al.*, 1974*b*; Tye, 1976). Our data indicate that this is not the case. We propose instead that a packaging sequence begins when the product of gene *3* interacts with a packaging initiation site, with the result that the concatemer is cleaved at *pac*. Such initiation events would occur randomly along the concatemer with a probability of about one-third for each *pac* site. Several headful sequences could initiate on a single concatemer.

λ and P22 DNA packaging begin in the same genetic region and depend on the acitivity of genes of equivalent map location. Both phages package DNA in short sequences of headfuls, with sequential headfuls forming along the concatemer in the same genetic direction. The two DNA packaging mechanisms differ principally in the requirements for the second cleavage that completes maturation of a linear DNA molecule. λ requires a specific nucleotide sequence to make this cut; P22 does not. The similarity of λ and P22 DNA packaging is further illustrated by the fact that encapsulation of excision-defective prophage DNA is identical for P22 and λ, except that λ cannot cleave bacterial DNA after packaging it into the phage head and P22 can (Sternberg & Weisberg, 1975; Weaver & Levine, 1978).

Interesting aspects of the P22 DNA maturation process remain obscure. What events initiate a packaging sequence? Why do packaging sequences begin at only one-third of the *pac* sites? How does encapsulation of DNA at the packaging initiation site differ from encapsulation of the second headful in the sequence? How do non-specific DNA cleavages occur? Does the same nuclease perform both nucleotide sequence-specific and non-specific DNA cleavages? *Eco*RI cleavage of P22 DNA provides a simple and sensitive experimental tool to study P22 DNA packaging. We are currently utilizing these methods to study mutants of P22 defective in packaging to learn more about the mechanism of P22 DNA maturation.

David Botstein and collaborators generously provided the insertion and deletion derivatives of P22 on which this work depends. We thank Tony Weighous for outstanding technical assistance, and Robert J. DeLeys for help with densitometric analysis. We also thank Steven Weaver and Myron Levine for access to unpublished data, and William Folk, David Friedman and Myron Levine for criticism of the manuscript. This work was supported by a grant from the National Institutes of Health (grant no. AI-12369).

REFERENCES

Botstein, D. (1968). *J. Mol. Biol.* **34**, 621–641.
Botstein, D. & Levine, M. (1968). *J. Mol. Biol.* **34**, 643–654.
Botstein, D., Chan, R. K. & Waddell, C. H. (1972). *Virology*, **49**, 268–282.
Botstein, D., Waddell, C. & King, J. (1973). *J. Mol. Biol.* **80**, 669–695.
Chan, R. K. (1974). Ph.D. thesis, Massachusetts Institute of Technology.
Chan, R. K. & Botstein, D. (1976). *Genetics*, **83**, 433–458.
Chan, R. K., Botstein, D., Watanabe, T. & Ogata, Y. (1972). *Virology*, **50**, 883–898.
DeLeys, R. J. & Jackson, D. A. (1976). *Nucl. Acids Res.* **3**, 641–652.
Denhardt, D. T. (1966). *Biochem. Biophys. Res. Commun.* **23**, 641–646.
DeVries, F. A. J., Collins, C. J. & Jackson, D. A. (1976). *Biochim. Biophys. Acta*, **435**, 213–227.
Emmons, S. W. (1974). *J. Mol. Biol.* **83**, 511–525.
Feiss, M. & Bublitz, A. (1975). *J. Mol. Biol.* **94**, 583–594.

Helling, R. B., Goodman, H. M. & Boyer, H. W. (1974). *J. Virol.* **14**, 1235–1244.
Hilliker, S. & Botstein, D. (1976). *J. Mol. Biol.* **106**, 537–566.
Jackson, E. N., Miller, H. I. & Adams, J. L. (1978). *J. Mol. Biol.* **118**, 347–363.
Jessop, A. P. (1976). *Genetics*, **83**, 459–475.
Raj, A. S., Raj, A. Y. & Schmieger, H. (1974). *Mol. Gen. Genet.* **135**, 175–184.
Rhoades, M., MacHattie, L. A. & Thomas, C. A. Jr (1968). *J. Mol. Biol.* **37**, 21–40.
Skalka, A. (1971). In *The Bacteriophage Lambda* (Hershey, A. D., ed.), pp. 535–547, Cold Spring Harbor Press, New York.
Smith, H. O. & Levine, M. L. (1964). *Proc. Nat. Acad. Sci., U.S.A.* **52**, 356–363.
Sternberg, N. & Weisberg, R. (1975). *Nature (London)*, **256**, 97–103.
Streisinger, G., Emrich, J. & Stahl, M. M. (1967). *Proc. Nat. Acad. Sci., U.S.A.* **57**, 292–295.
Thomas, M. & Davis, R. W. (1975). *J. Mol. Biol.* **91**, 315–328.
Tye, B. K. (1976). *J. Mol. Biol.* **100**, 421–426.
Tye, B. K., Chan, R. K. & Botstein, D. (1974*a*). *J. Mol. Biol.* **85**, 485–500.
Tye, B. K., Huberman, J. A. & Botstein, D. (1974*b*). *J. Mol. Biol.* **85**, 501–532.
Wang, J. C. & Kaiser, A. D. (1973). *Nature New Biol.* **241**, 16–17.
Watanabe, T., Ogata, Y., Chan, R. K. & Botstein, D. (1972). *Virology*, **50**, 874–882.
Weaver, S. & Levine, M. (1978). *J. Mol. Biol.* **118**, 389–411.